Int J CARS (2009) 4:307–315
DOI 10.1007/s11548-009-0296-z

ORIGINAL ARTICLE

Robot-assisted catheter manipulation for intracardiac navigation

Yusof Ganji · Farrokh Janabi-Sharifi · Asim N. Cheema

Received: 29 October 2008 / Accepted: 24 February 2009 / Published online: 13 March 2009

Abstract
Objective Manual navigation of intracardiac steerable catheters is inaccurate, requires dexterity for efficient manipulation of the catheter, and exposes the interventionalist to ionizing radiation. The objective of this research is to develop a system that replaces the interventionalists's hands in catheter manipulation for accurate and semi-automatic tele-navigation of catheters.
Methods Based on a proposed kinematic model for the distal shaft of the catheter, a system has been developed for assisted navigation of intracardiac catheters. When the distal shaft of the catheter lies inside a cardiac chamber, a robotic apparatus is utilized for automatic steering of the catheter tip to reach designated targets within the chamber.
Results The catheter modeling was validated through the experiments on three swine. The robotic system could navigate the catheter tip to designated targets with a mean distance of 6.53 mm from the target.
Conclusion Preliminary in vivo studies demonstrate the feasible application of the system in catheter navigation and the validity of catheter modeling and control strategies.

Y. Ganji (✉)
Department of Electrical and Computer Engineering,
University of Waterloo, Waterloo, ON N2L 3G1, Canada
e-mail: yganji@ieee.org

F. Janabi-Sharifi
Department of Mechanical and Industrial Engineering,
Ryerson University, Toronto, ON M5B 2K3, Canada

A. N. Cheema
St. Michael's Hospital, Toronto, ON M5B 1W8, Canada

A. N. Cheema
Division of Cardiology, University of Toronto,
Toronto, ON M5G 2C4, Canada

Keywords Catheter · Intracardiac navigation · Robot-assisted manipulation · Modeling

Introduction

Steerable electrophysiology (EP) catheters are widely used in the interventional treatment of cardiac arrhythmias. In an EP session, the interventionalist or electrophysiologist manipulates the catheter handle and its steering knob to bring the catheter electrodes or ablation cap, at the distal shaft of the catheter, in contact with the intracardiac anatomy. Catheter manipulations result in translation, twist, and deflection of the distal shaft, repositioning the shaft inside the cardiac chambers. The major goal of the manipulations is to position the shaft such that a stable contact with the endocardium is achieved in order to conduct EP study and ablation. However, the flexible catheter shaft is subject to intracardiac blood flow and cardiac contractions, and the transfer of the manipulations at the handle or proximal section to the shaft is generally non-linear. Consequently, successful positioning of the catheter is often achieved after repeated attempts depending on the experience, skills, and fatigue of the interventionalist. As a result, catheter-based procedures could entail prolonged exposure of the interventionalists and the patients to ionizing radiation of fluoroscopy.

To assist catheter steering and navigation, two commercial systems have been developed. Niobe® (Stereotaxis, St. Louis, MO) realizes magnetic navigation [1,2] using a special magnetic catheter. In this system, two permanent magnets are placed on the sides of patient table and the catheter is navigated inside their magnetic field. To deploy Niobe®, the catheterization lab must be magnetically compatible with the system. Niobe®cannot be deployed on patients that have metallic implants as well. Sensei™ (Hansen Medical,

Mountain View, CA) is a robotic catheter control system [3,4] that uses two steerable sheaths through which an EP catheter is deployed. Both Niobe®and Sensei™systems provide for remote manipulation of the catheter, thus reducing the exposure to the radiation of fluoroscopy for the interventionalists. However, the cost of such systems could be a prohibitive factor in their utilization. In academia, there have been attempts to build steerable catheters utilizing micro-hydraulic actuators [5–7], and shape memory alloys [8,9]. In such catheters, the actuators are collocated with and housed inside the deflectable shaft. These systems rely on specialized catheters or sheaths along with their actuation mechanisms to realize catheter navigation.

To facilitate the manipulation and navigation of the catheter, without the bulk of support systems that entail operating room customizations and added costs, Cercenelli et al. [10] have mounted a typical catheter on a robotic system that enables motorized manipulation of the catheter and repetition of recorded manipulations. However, to navigate a commercially available catheter automatically in an economical way, no publication was found in the literature.

The motivation for this research is to facilitate the navigation of the catheter tip inside the cardiac anatomy automatically, thus improving the precision of navigation and reducing the fatigue incurred. The second motivation is to enable telemanipulation of the catheter, and to reduce the exposure of the interventionalists to X-ray radiation. To this end, the authors have characterized and modeled the distal shaft of steerable catheters in their previous works [11–13]. Based on the model, a robotic system was developed that allows semi-automatic positioning and navigation of the catheter. In this paper, the catheter model is reviewed and the robotic system and its control strategy is presented. In vivo experiments on three pigs are also presented that validate the catheter modeling and demonstrate the feasibility of automatic navigation to reach intra-atrial landmarks.

Materials and methods

Kinematic model of distal shaft

The distal shaft of the catheter can be considered as a single-section extrinsic planar continuum robot, as defined in [14]. A continuum robot is a flexible manipulator that bends along its length and does not have distinct links and joints. The catheter is also extrinsic as the actuators are not collocated with the distal shaft. Based on the principle proposed by Hannan, Walker and Jones [15,16], and as described in [12], we model the distal shaft with rigid links and joints. The model along with its assigned Denavit–Hartenberg (D–H) frames [17] is depicted in Fig. 1.

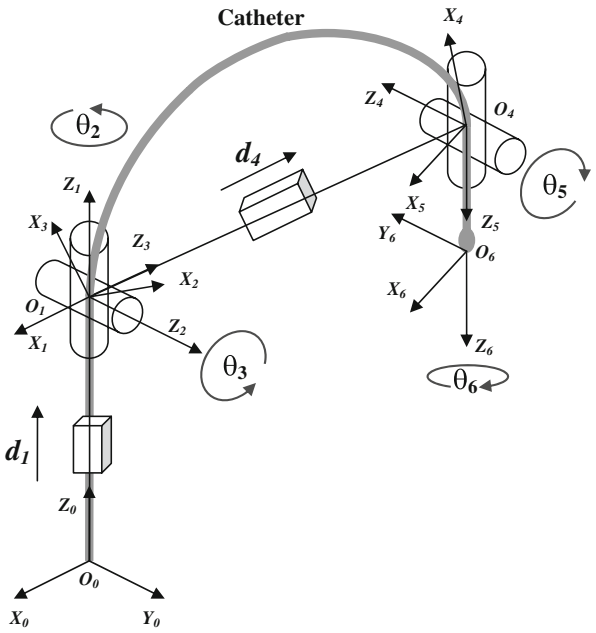

Fig. 1 Catheter model and the assigned D–H coordinate frames

It is assumed that the catheter bends with zero torsion, and with constant curvature, as defined in differential geometry [18]. Zero torsion implies planar deflection, and the constant curvature means that the bending section always takes the shape of a circular arc. With these two assumptions, and with reference to Fig. 1, to reach from the base of the distal shaft (O_1) to the end of the bending section (O_4) in three-dimensional space, two rotations followed by one translation, and followed by two rotations are required. As a result, the catheter model will be composed of three sections:

1. O_0O_1. This section constitutes the virtual base of the distal shaft. The translation of the distal shaft is represented by a prismatic joint. As the distal shaft is always aligned with the catheter body just below the distal shaft base (O_1), the prismatic joint can suitably model the differential motion of the distal shaft base, assuming the coordinate frames 0 and 1 are parallel. It is noted that as long as the displacement of the body (d_1) and not the actual position of the model base is of concern, the prismatic joint can represent the displacements.
2. O_1O_4. The bending section of the distal shaft is represented by two revolute joints, one prismatic joint and two revolute joints that together accomplish the preceding two rotations, followed by one translation, and followed by two rotations. Consequently, the flexible bending section is modeled by rigid components.
3. O_4O_6. This section represents the distal end of the catheter that is almost rigid. It houses a number of electrocardiogram (ECG) electrodes and the ablation cap. The

Table 1 Denavit–Hartenberg parameters

Link	a	α	d	θ	Joint variable
1	0	0°	d_1	0°	d_1
2	0	90°	0	θ_2	θ_2
3	0	90°	0	$90° + \theta_3$	θ_3
4	0	90°	d_4	0°	d_4
5	0	90°	0	$180° + \theta_5$	θ_5
6	0	90°	0	θ_6	θ_6
7	0	0°	d_7	0°	d_7

The distal end is unnumbered

ablation cap is considered the end-effector of the manipulator model. The length of this section is an intrinsic parameter of the catheter and is constant.

Based on the assigned D–H coordinate frames illustrated in Fig. 1, the D–H parameters are summarized in Table 1. The curvature constancy and the coupling between parameters yield $\theta_5 = 90° - \theta_3$ and $\theta_6 = 180° - \theta_2$. The constant length of the distal end (O_4O_6) is denoted by d_7.

Using Table 1, the forward kinematics of the model is calculated and the position of the catheter tip with respect to the virtual base O_0 is found, as follows.

$$\begin{bmatrix} x \\ y \\ z \end{bmatrix} = \begin{bmatrix} \cos\theta_2(d_4\cos\theta_3 + d_7\sin 2\theta_3) \\ \sin\theta_2(d_4\cos\theta_3 + d_7\sin 2\theta_3) \\ d_1 + d_4\sin\theta_3 - d_7\cos 2\theta_3 \end{bmatrix}. \quad (1)$$

Constant curvature deflection of the catheters means that the parameters θ_3 and d_4 are coupled. The coupling relationship follows [12].

$$d_4 = \frac{L}{\frac{\pi}{2} - \theta_3}\cos\theta_3. \quad (2)$$

Using (2), the number of variables in (1) reduces to three parameters d_1, θ_2 and θ_3. This result will be used in Jacobian based control, as described in the next section.

Inverse kinematic control

The objective of the system is to control the position of the tip of the catheter. The catheter is kinematically modeled as a continuum manipulator and to apply the model to position control, inverse kinematics is the available choice. The catheter's virtual joint parameters d_1, θ_2 and θ_3 are actuated at the handle. However, the catheter is not composed of rigid links and direct measurement of virtual joint parameters is not possible. To control the catheter tip position in lieu of uncertain joint parameters, operation/task space control is the practical choice, as opposed to joint space control [17].

To implement any inverse kinematic control strategy, Jacobian matrix is the required tool. Based on the position vector in (1) and after eliminating variable d_4 using (2), the analytical position Jacobian (J) can be calculated.

Among inverse kinematic control strategies, Jacobian-transpose method is not a suitable choice for real-time control of catheter position in the intracardiac setting, due to its low convergence speed and sensitivity to noise. Given that the distal shaft Jacobian is a square matrix, the Jacobian inverse is the method of choice for this purpose. To resolve the Jacobian-inverse unstability issue near singularities, damped least square method [19] is utilized. As a result, the control law can be formalized by

$$[\delta d_1 \quad \delta\theta_2 \quad \delta\theta_3]^{\mathrm{T}} = J^{\mathrm{T}}(JJ^{\mathrm{T}} + \lambda I)^{-1}[x_{\mathrm{e}} \quad y_{\mathrm{e}} \quad z_{\mathrm{e}}]^{\mathrm{T}}, \quad (3)$$

where x_{e}, y_{e} and z_{e} constitute the error vector in catheter tip positioning and λ is the damping factor computed by

$$\lambda = \begin{cases} \lambda_0(1 - \frac{w}{w_{\mathrm{t}}})^2 & w < w_{\mathrm{t}} \\ 0 & w \geq w_{\mathrm{t}} \end{cases} \quad (4)$$

where $w = \det(J)$ and w_{t} is the threshold below which the catheter is assumed to be near singular configurations [20].

System setup

The system developed for catheter navigation is illustrated in Fig. 2. The description of the components follows.

Catheter and its position

The catheter model in "Kinematic model of distal shaft" can be applied to any unidirectional or symmetric bidirectional ablation catheter. A bidirectional and symmetrical steerable ablation catheter, SteeroCath-T (BostonScientific, Natick, MA) was adopted for experimental validation of the proposed model and the position control strategy. The adopted catheter's diameter is 7 French and its tip's diameter is 8 French. This catheter is 110 cm long.

To track the positions of the distal shaft of the catheter, the Aurora electromagnetic tracking system (NDI, Waterloo, ON, Canada) was deployed. Aurora provides position and orientation (pose) of its small sensors that are placed in its electromagnetic field generator's measurement volume. For the experiments, two sensor coils were used to track the catheter position and to estimate the catheter model's joint parameters. One sensor coil was attached to the base of the distal shaft (at O_1 in Fig. 1) and the other sensor was attached to the tip section (O_4O_6 in Fig. 1). Figure 3 shows a close-up of the sensors attached to the distal shaft. The sensors were glued to the shaft using contact cement and then were rubber-coated for a better bond and seal. Aurora provides position readings of the sensors with submillimetre accuracy at up to 40 Hz update rate. In order to match the model with

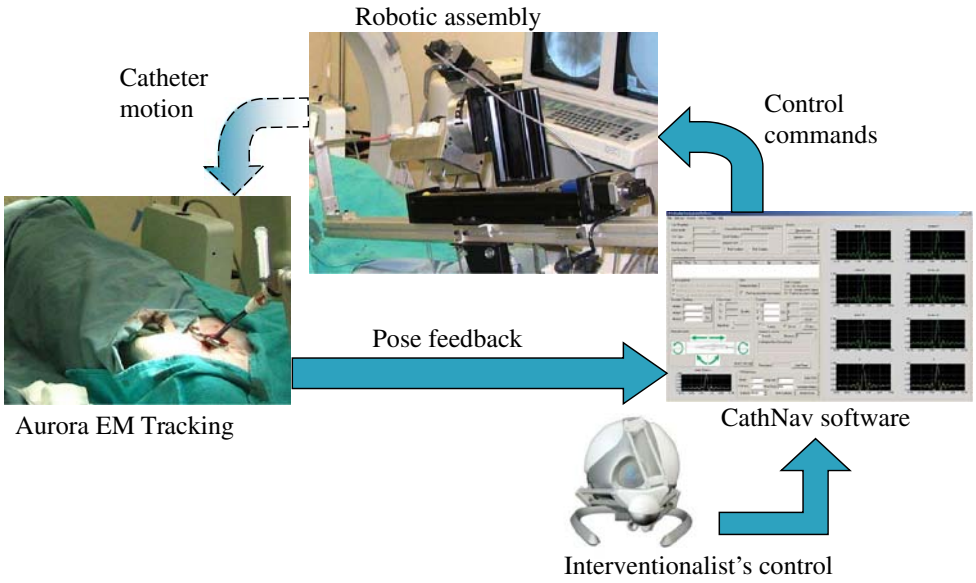

Fig. 2 An overview of system components and their interactions

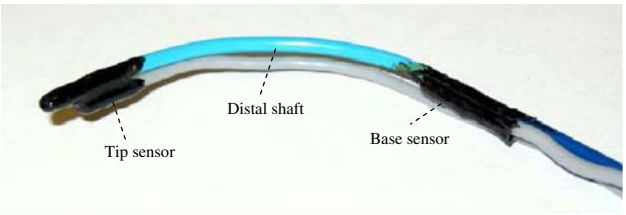

Fig. 3 Aurora sensors attached to the distal shaft of the catheter

catheter's actual position, the pose readings from the sensors were calibrated so that the base sensor represented O_1 and the readings from the tip sensor yielded the position of O_4 and O_6. A sheath covered the catheter body and sensor wires that ran along the catheter body in parallel. The added asymmetric thickness of the sensors and the sheath, increased the tracked catheter's diameter to 15 to 18 French. The sheath-covered tracked catheter will be referred to as catheter assembly henceforth.

Robotic assembly

A three degrees of freedom (DOF) robot was designed and constructed to mimic the manipulations an interventionalist performs on the catheter handle. The manipulations include insertion/retraction of the catheter, twisting the catheter handle or proximal body to induce some rotation at the distal shaft, and deflecting the distal shaft using the steering knob at the handle. The robot was assembled of one linear stage for insertion/retraction of the catheter and two rotary stages, to twist and deflect the catheter. The robot was mounted on a stand that allowed the adjustment of catheter's entry angle with respect to the port of entry at femoral vein. The catheter's proximal end was passed through an telescopic tubing that kept the catheter body, lying outside the introducer sheath, straight. This allowed better transfer of translation and torque actuated by the robot at the handle to the distal section of the catheter.

Computer control system

A software platform, named CathNav, was developed in Microsoft Visual C++ environment to validate catheter modeling and to realize real-time position control of the catheter. The platform interfaced with Aurora and robot motor controllers and drives (VXM, Velmex, Bloomfield, NY) through RS-232 serial interfaces. For vector, quaternion and matrix processing, VL Vector Libraries [21] were utilized. Using CathNav, the sensor readings were calibrated, filtered, and recorded. CathNav also provided the user interface (UI) for the interventionalist to control and manipulate the catheter. Through the UI, the interventionalist could command the robot to push or pull, twist or deflect the catheter as desired.

In everyday operations, the interventionalist relies on his or her skills and experience to find out how to manipulate the catheter in order to achieve tip motion in a desired direction and to reach a specific target position inside the heart. The control algorithm, outlined in "Inverse kinematic control", was implemented in CathNav to achieve three-dimensional (3D) control of the catheter tip position relieving the interventionalist from having to manipulate the individual DOFs at the handle. A 3D haptic device (Falcon, Novint Technologies Inc., Albuquerque, NM) was integrated with the system to let the interventionalist intuitively direct the catheter in anterior/posterior, superior/inferior and left/right directions.

To automate the process of moving the catheter tip toward a specific position, a path planning algorithm was implemented on top of the controller, to devise the straight path trajectory for the catheter from its instantaneous position to a target position. The path planner was responsible for automated navigation of the catheter tip to reach a given target by issuing new set points to the controller. For safety reasons, the operator could intervene the automatic manipulation whenever necessary.

Experiments setup

To study the feasibility of the application of the system in actual interventions, the system was tested and validated on three porcine subjects in the research vivarium in St. Michael's Hospital in Toronto, ON, Canada. Porcine subjects were utilized due to their long established tradition as a viable model, for testing human intracardiac devices. Swine are similar in size, anatomy and physiology to human making them ideal candidates for human intracardiac catheterization. The experiment protocol was approved by the hospital's Animal Care And Use Committee, in accordance with Canadian Council On Animal Care guidelines.

Each subject was sedated with a cocktail of xylazine (2 mg/kg), ketamine (20 mg/ml) and one ampoule of Atropine (0.6 mg/ml). After 15 min, the swine was immobilized, allowing for it to be weighed and transferred to the pre-op room. Then it was masked with a gas inhalant of isofluorane at 5%. A 22G angiocatheter was placed in the ear and IV fluids (0.9 ml NaCl) was started on a slow drip. The subject was then placed in dorsal recumbency and intubated for artificial respiration. After intubation, it was transferred to the operating room and ECG electrodes were attached for monitoring the electrocardiogram. During the procedure, the subject was maintained on 2.5–3% isofluorane. A femoral venous cutdown was done on both hind limbs, as well as a jugular cutdown on the neck. After the procedure, the swine was sacrificed with a lethal intravenous (IV) injection of sodium pentobarbital (540 mg/ml).

The catheter assembly was deployed on the robotic assembly and was inserted through a 22-French introducer sheath (Cook Medical Inc., Bloomington, IN) into the right femoral vein and was threaded into the right atrium (RA). The catheter assembly was introduced into RA manually prior to being mounted on the robot. The Aurora field generator was placed beside the swine chest so that the distal shaft of the catheter (with two attached Aurora sensors) in the RA could be tracked within the Aurora's measurement volume. A third Aurora sensor was introduced through the left jugular vein and threaded into the RA as well. This sensor could be positioned at desired landmarks in RA. The sensor position was the target of the navigation experiments. This sensor will be referred to as the reference sensor henceforward. At any instant, the distance vector between the catheter assembly tip and the reference sensor was presented through the software UI to assist the operator in controlling the catheter position.

The operation was monitored under fluoroscopy (OEC Series 9800 cardiac mobile C-Arm, GE Healthcare Technologies, Waukesha, WI). For better visualization of the navigation process, intracardiac echocardiography (ICE) was used as well. An ICE catheter (Acuson AcuNav, Siemens AG Medical Solutions, Erlangen, Germany) was introduced through the left femoral vein into the RA. ICE images provided a better view of where the catheter assembly and the reference sensor were positioned relative to the intra-atrial anatomy.

Results

Model validation

In order to verify that the distal shaft model can match the reality of distal shaft shape, two scenarios were implemented and tested on the animals. In each scenario, the catheter went through a pre-programmed motion and its position profile measured with Aurora sensors was recorded. The model parameters were found and the model's position vector (1) was compared with the actual position measurements. The difference between model position vector and the recorded tip position was defined as the modeling error. The error value was the basis in calculating the accuracy and precision of the modeling in vivo. Accuracy was defined as the error mean value (μ) and precision was defined as the standard deviation of the error (σ). The error value was calculated for the three coordinates of the position vector (1), with respect to O_0 coordinate system in Fig. 1. The overall error was also calculated as the Euclidean distance between the measured position and the model estimation of the position.

Deflection

In this experiment, the distal shaft was deflected by turning the steering knob at the handle in 1 degree steps. The steering knob was turned from 0 degrees up to 40 degrees and then turned back to zero. This back and forth rotation was repeated 20 times, resulting in 1600 position measurements for each animal. Table 2 presents the accuracy and precision figures.

Combined twist and deflection

In this experiment, the distal shaft was deflected and twisted at the same time. The steering knob was turned from zero at 1 degree steps up to 36 degrees and then turned back to zero. The handle was also twisted similarly at 10 degree steps up

Table 2 Modeling error in deflection experiments

	μ_x	σ_x	μ_y	σ_y	μ_z	σ_z	μ	σ
1	1.78	0.69	0.64	0.28	2.66	2.06	3.40	1.99
2	2.35	0.84	−1.88	0.50	0.63	2.59	4.10	0.58
3	1.81	0.21	0.59	0.15	1.18	0.22	2.26	0.28

Mean (μ) and standard deviation (σ) of the error are presented for x, y, z coordinates in addition to the Euclidean distance between the model and the measured position, denoted without the coordinate subscripts. All measurements are in millimetre

Table 3 Modeling error in combined twist and deflection experiments

	μ_x	σ_x	μ_y	σ_y	μ_z	σ_z	μ	σ
1	2.15	0.76	0.58	0.46	2.42	1.68	3.41	1.68
2	0.67	1.42	−1.88	1.28	2.14	1.35	3.50	1.36
3	1.17	2.11	−2.70	0.94	3.01	1.51	4.81	1.47

Mean (μ) and standard deviation (σ) of the error are presented for x, y, z coordinates in addition to the Euclidean distance between the model and the measured position, denoted without the coordinate subscripts. All measurements are in millimetre

to 360 degrees. This combined twist and deflection trajectory was traversed twenty times resulting in 1,440 position measurements for each animal. Table 3 summarizes the error figures.

The position errors measured in the experiments are generally under 5 mm. This indicates that the proposed model can be utilized as an approximation of the catheter's distal shaft shape and to parameterize the position vector of the tip. The model remains valid in the presence of intra-atrial pressure levels and under the displacements induced by respiration and cardiac contractions. Consecutively, the model is deployed to control the position of the catheter and to navigate the catheter inside the atrium. It is noted that the model does not account for any interaction of the distal shaft with the intracardiac anatomy. As a result, when the shaft comes into contact with the endocardium, depending on the dynamics of the contact, the model's accuracy can be undermined. As demonstrated in the subsequent section, the control law (3) provides the basis for the successful navigation of the catheter, unless contact forces deform the catheter to the extent that the curvature constancy or zero torsion assumptions are strongly violated.

Navigation validation

To validate the capability of the system in navigating the catheter tip to desired positions, the reference sensor was positioned on three landmarks in the right atrium (low RA, high RA and Tricuspid Valve Annulus) in each animal. The catheter assembly was positioned so that the tip was in mid-atrium at the beginning of each navigation task. The system was commanded to direct the tip toward the reference sensor automatically till it reached and touched the reference sensor. The navigation task was ended when the supervising interventionalist was satisfied with the position of the catheter tip at the landmark, viewed under fluoroscopy. The initial and final distance between the catheter tip and the reference sensor were recorded along with the duration of the navigation task. The system was then commanded to take the catheter back to the initial mid-atrial position by "undoing" all the manipulations performed on the catheter during the navigation. Through UI controls and the haptic interface, the catheter could be positioned manually at the mid-atrium if the catheter did not move completely back to the original position, due to the inherent hysteresis in the transfer of actuation at the handle to the distal shaft, especially when the catheter is twisted. For each landmark, the navigation manoeuvre was repeated five times. The trajectory planned for the catheter tip was a straight line between the instantaneous catheter tip position and the reference sensor position. This scheme was supposed to yield the shortest navigation time.

Figure 4 presents the initial and final configuration of the catheter assembly and the reference sensor in a sample navigation. As seen in the figure, the catheter tip touches the reference sensor at the end of navigation. Figure 5 illustrates a sample of distance readings between the catheter tip and the reference sensor in a high RA navigation. In this figure, the successful navigation of the catheter in the presence of the disturbances due to the continuous beating cycle is visible. The ideal path to reach the reference sensor and the actual path taken due to disturbances and uncertainties is depicted in the figure. The motion induced on the reference sensor by the cardiac contraction/relaxation cycle is clearly visible by the variations in the unfiltered distance readings.

Table 4 presents the outcome of the automated navigation for each landmark. Except for one case where the catheter tip was stuck on its way to the Tricuspid Valve Annulus, the navigation tasks were all conducted successfully. The final distance between the reference sensor and the tip was generally below 10 mm with an average of 6.53 mm. This means even though the catheter reached at the desired target according to the interventionalist, there was still some distance to the reference sensor. This was partly attributed to the length of sensor coil (9 mm), and to the dynamics of the contact between the catheter tip, the reference sensor and intra-atrial anatomy. The typical navigation time was between 30 and 60 s.

Discussion

The model proposed for distal shaft kinematics was validated through in vivo experiments. Based on the model, a control algorithm was implemented and tested on the system and a path planning algorithm was developed to navigate

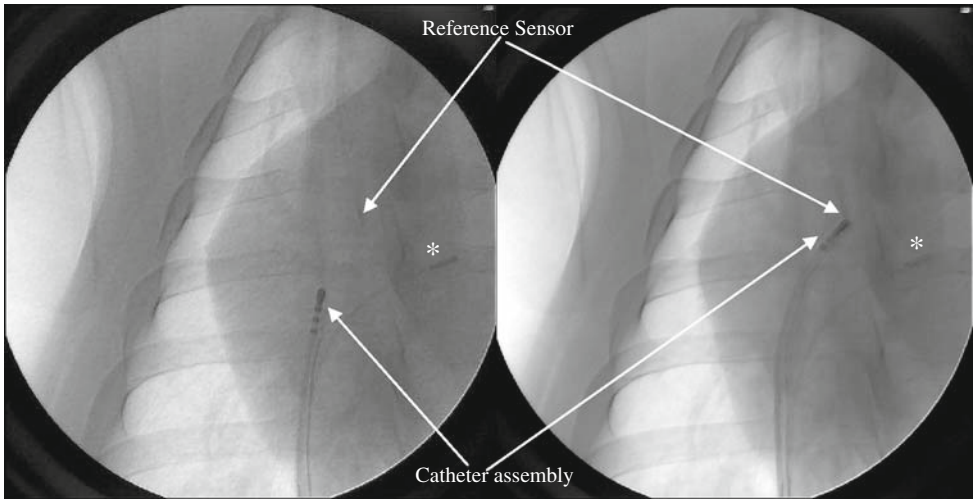

Fig. 4 Initial (*left*) and final (*right*) positioning of the catheter assembly in navigation from mid-RA to high RA, as captured by fluoroscopy. The ICE catheter is marked with an *asterisk*

the catheter tip from its instantaneous position to the desired position. The experiments demonstrated that the navigation is feasible in actual operations inside the right atrium.

In the experiments, there were instances where the distal shaft was stuck on its way to the reference sensor. Such obstacles once resulted in a failed navigation attempt while in other instances the system managed to release the catheter. This resulted in variations in the duration of navigation tasks as indicated by the large σ_t in Table 4. For safety reasons, CathNav stops robotic manipulation when the tip configuration does not change after multiple attempts. The intracardiac anatomical features are obstacles that the catheter should avoid on its path. The path planned in CathNav software is a straight line from the catheter tip to the target position. To enhance the navigation capability, the system should accommodate different curves as navigation path of the tip to avoid anatomical obstacles.

In addition to anatomical obstacles, the proposed rigid model for the catheter can lose its accuracy when contact forces with the endocardium affect the shape of the distal shaft significantly. Based on the elastic beam theory, the model's rigid links can be replaced with flexible beams, modeling the distal shaft as a flexible manipulator. As a result, the model could include the physics of elastic bending due to contact with anatomy, providing for navigation to more difficult to reach landmarks on the endocardium.

In the experiments, the haptic interface demonstrated an alternative to classical twist, push/pull, and bend paradigm for catheter manipulation at the handle to a more intuitive superior/inferior, posterior/anterior, left/right paradigm at the tip where actual navigation takes place. However, it was learned that relying on fluoroscopy and ICE proves insufficient for manual navigation of the catheter through the haptic interface. While the interface provides a significant improvement in navigation approach, a graphical visualization is required to display the cardiac anatomy and the distal shaft position registered on the anatomy. The interventionalists can then conveniently control the catheter tip position through the system.

In any automated navigation system, safety is of crucial importance. For intracardiac navigation, the force that the distal shaft and especially the tip exerts on the myocardium determines the safety of manoeuvres. A force/tactile feedback from the distal shaft is a pre-requisite for the deployment of such a system in real human operations. The authors plan to embed a tactile safety feature in the catheter.

The catheter assembly with the attached Aurora sensors increases the diameter of the catheter, and limits the deflection of the distal shaft. It also limits the translation of torque from the proximal section to the distal shaft. Ideally, the sensors could be embedded inside the catheter, thus allowing better manoeuvrability of the tip. In addition, it is expected that by inclusion of better actuators for the robot, the navigation time can be reduced.

In practice, the robotic system will only use electromagnetic tracking for its operation. The supervising interventionalist will rely on his modality of choice (e.g., fluoroscopy or ultrasound) to manage and control the system. In the experiments, an electromagnetic sensor was deployed as the target point for automatic navigation. In practice, such a target point is not readily available. One way to provide a target point is to register fluoroscopic images in the electromagnetic coordinate system. In this approach, the GUI of the system can provide the interface to mark the target point on the images and the registered image could yield the target position in the coordinates. The sensors attached to the catheter can be used as fiducial markers in the registration process. The authors plan to develop a methodology for this registration. In addition to automatic navigation which requires an elaborate system for target integration, the system already provides the enhanced navigation of the catheter using the haptic and graphical interfaces.

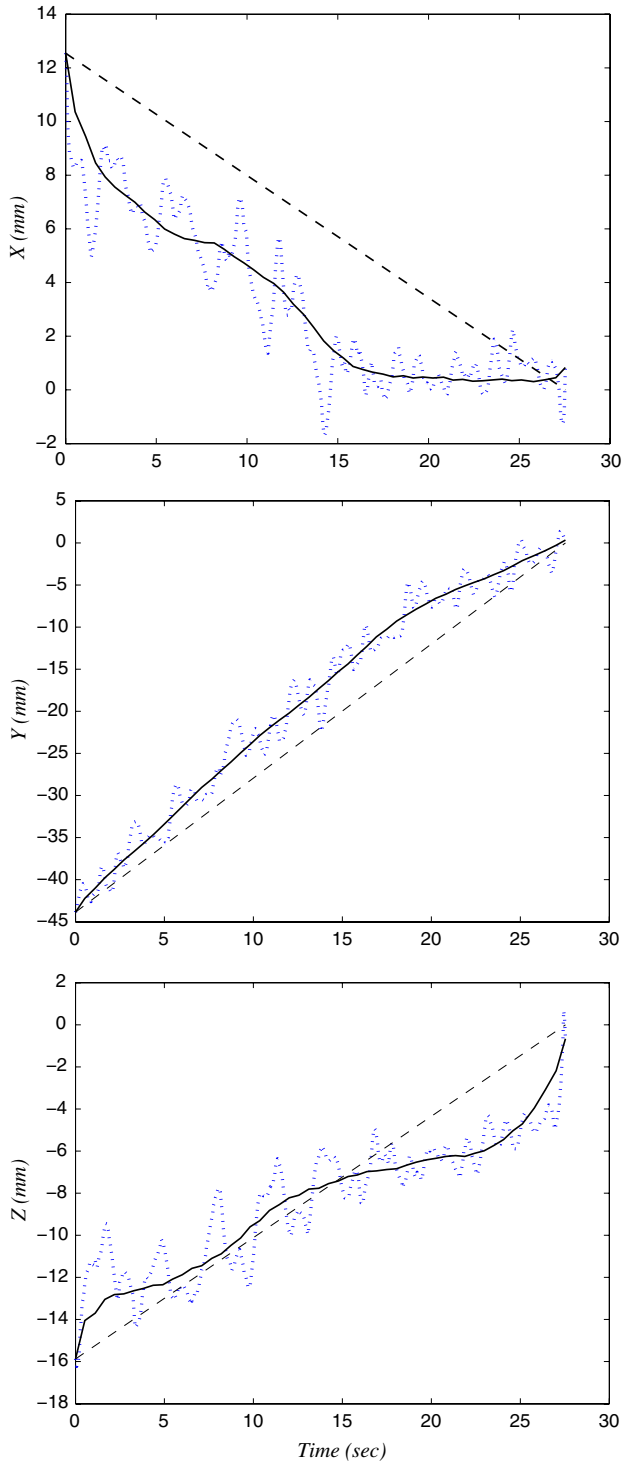

Fig. 5 X, Y and Z coordinates of the distance vector between the catheter tip and the reference sensor. *Dashed line* depicts the ideal straight path to the reference sensor. *Solid line* depicts the actual path the controller realized in navigating the catheter. *Dotted line* represents the distance readings, with unfiltered cardiac cycle disturbances

Finally, a brief comparison with the competing technologies [22] already in clinical practice is in order. Sensei™uses a proprietary steerable dual sheath system and achieves a stable control over the passive catheter position that is threaded through the sheath. Sensei™provides enhanced but not automatic navigation. Our navigation system provides a simpler method to achieve semi-automatic navigation without additional sheaths. Both robotic systems, however, require extra safety measures to avoid traumatic navigation. On the other hand, Niobe®realizes magnetic navigation of a proprietary magnetic catheter and performs semi-automated mapping. Niobe®is a very safe solution with no risk of cardiac perforation but it requires a complete catheterization lab customization. In short, the developed system provides the advantage of automatic navigation with less complexity and cost compared to the existing technologies. However, the system requires manual insertion of the catheter prior to navigation in contrast to both systems. In addition, to be adopted for clinical practice, the catheter will require the Aurora sensors to be embedded inside the steerable catheter. Lastly, a performance comparison with manual navigation is required to assess the merits and shortcomings of the developed system. This is the subject of the authors' future work.

Table 4 Navigation performance in terms of initial and final distance between the catheter tip and the reference sensor and the duration for the system to perform the navigation automatically

Landmark	Initial distance (mm)		Final distance (mm)		Duration (s)	
	μ_i	σ_i	μ_f	σ_f	μ_t	σ_t
High RA	37	3.25	5.02	2.21	45.91	15.29
Low RA	30.91	2.76	7.38	2.93	46.16	18.34
TVA	33.45	1.65	9.34	1.25	36.95	16.66

RA right atrium, *TVA* tricuspid valve annulus

Conclusion

In this paper, the distal shaft of steerable catheters was modeled as a continuum manipulator composed of rigid links and joints. The kinematics of the model was presented and a control strategy for position control of the catheter tip, based on the proposed model was devised. To validate the modeling and control methods in vivo, a robotic system to replace the interventionalist's hand in catheter manipulation was constructed. The catheter handle was mounted on the robot and its distal shaft was tracked using the Aurora electromagnetic tracking system. A software platform was also developed to control the robotic assembly for enhanced navigation of the catheter. The software provided the UI and a haptic interface for manipulation and navigation of the catheter.

The animal experiments verified that the catheter modeling provides acceptable accuracy and precision in the estimation of the catheter tip position. The experiments also verified the feasibility of automatic navigation of the catheter from

a given position to a desired position marked using a reference sensor. Based on the experimental results, the authors will extend the catheter's rigid model to account for deformations due to contact forces, in order to prepare the system for navigation in the presence of anatomical obstacles on catheter's path.

Acknowledgments The authors wish to thank Mr. Joseph B. Koblish, with Boston Scientific Corp. EP Technologies, for providing catheter samples and information on the mechanical construction of the catheters, and Mr. Jeff Stanley, with NDI medical research, for his continued support. NDI's contribution by lending the Aurora system is acknowledged. The contributions of Mr. Devin Ostrom, technical officer in Ryerson University, in robotic assembly design and machining is highly appreciated. The cooperation of Ms. Melissa Mitchel, with the research vivarium in St. Michael's hospital, is especially appreciated. This research was financially supported through Natural Sciences and Engineering Research Council of Canada (NSERC) Discovery Grants 203060-02 and 203060-07.

References

1. Pappone C, Vicedomini G, Manguso F, Gugliotta F, Mazzone P, Gulletta S, Sora N, Sala S, Marzi A, Augello G, Livolsi L, Santagostino A, Santinelli V (2006) Robotic magnetic navigation for atrial fibrillation ablation. J Am Coll Cardiol 47(7):1390–1400
2. Armacost M, Adair J, Munger T, Viswanathan R, Creighton F, Curd D, Sehra R (2007) Accurate and reproducible target navigation with the stereotaxis Niobe® magnetic navigation system. J Cardiovasc Electrophysiol 18(s1):26–31
3. Saliba W, Reddy V, Wazni O, Cummings J, Burkhardt J, Haissaguerre M, Kautzner J, Peichl P, Neuzil P, Schibgilla V et al (2008) Atrial fibrillation ablation using a robotic catheter remote control system: Initial human experience and long-term follow-up results. J Am Coll Cardiol 51(25):2407–2411
4. Kanagaratnam P, Koa-Wing M, Wallace D, Goldenberg A, Peters N, Davies D (2008) Experience of robotic catheter ablation in humans using a novel remotely steerable catheter sheath. J Interv Card Electrophysiol 21(1):19–26
5. Ikuta K, Ichikawa H, Suzuki K, Yajima D (2006) Multi-degree of freedom hydraulic pressure driven safety active catheter. In: Proceedings of the IEEE international conference on robotics and automation (ICRA'06), Orlando, FL, pp 4161–4166
6. Haga Y, Muyari Y, Mineta T, Matsunaga T, Akahori H, Esashi M (2005) Small diameter hydraulic active bending catheter using laser processed super elastic alloy and silicone rubber tube. In: Proceedings of the IEEE/EMBS special topic conference on microtechnology in medicine and biology, Kahuku, Hawaii, pp 245–248
7. Bailly Y, Amirat Y (2005) Modeling and control of a hybrid continuum active catheter for aortic aneurysm treatment. In: Proceedings of the IEEE international conference on robotics and automation (ICRA'05), Barcelona, Spain, pp 924–929
8. Haga Y, Mineta T, Esashi M (2002) Active catheter, active guidewire and related sensor systems. In: Proceedings of World Automation Congress, vol 14, Orlando, FL, pp 291–296
9. Jayender J, Patel R (2007) Master-slave control of an active catheter instrumented with shape memory alloy actuators. In: Proceedings of the IEEE/RSJ international conference on intelligent robots and systems (IROS'07), San Diego, CA, pp 759–764
10. Cercenelli L, Marcelli E, Plicchi G (2007) Initial experience with a telerobotic system to remotely navigate and automatically reposition standard steerable ep catheters. ASAIO J 53(5):523–529
11. Ganji Y, Janabi-Sharifi F (2006) Catheter kinematics and control to enhance cardiac ablation. In: Proceedings of the SPIE, vol 6374, p 63740U
12. Ganji Y, Janabi-Sharifi F (2007) Kinematic characterization of a cardiac ablation catheter. In: Proceedings of the IEEE/RSJ international conference on intelligent robots and systems (IROS'07), San Diego, CA, pp 1876–1881
13. Ganji Y, Janabi-Sharifi F (2009) Catheter kinematics for intracardiac navigation. IEEE Trans Biomed Eng (in press)
14. Robinson G, Davies JBC (1999) Continuum robots: s state of the art. In: Proceedings of the IEEE international conference on robotics and automation (ICRA'99), Detroit, MI, pp 2849–2854
15. Hannan MW, Walker ID (2003) Kinematics and the implementation of an elephant's trunk manipulator and other continuum style robots. J Robot Syst 20(2):45–63
16. Jones BA, Walker ID (2006) Kinematics for multisection continuum robots. IEEE Trans Robot 22(1):43–55
17. Sciavicco L, Siciliano B (2000) Modelling and control of robot manipulators. 2nd edn. Springer, Heidelberg
18. Somasundaram D (2005) Differential geometry, a first course. Alpha Science International Ltd, UK
19. Deo A, Walker I (1995) Overview of damped least-squares methods for inverse kinematics of robot manipulators. J Intell Rob Syst 14(1):43–68
20. Nakamura Y, Hanafusa H (1986) Inverse kinematic solutions with singularity robustness for robot manipulator control. ASME J Dyn Syst Meas Control 108:163–171
21. Willmott AJ (2002) VL vector library. http://www.cs.cmu.edu/afs/cs/user/ajw/www/software/
22. Schmidt B, Chun KRJ, Tilz RR, Koektuerk B, Ouyang F, Kuck KH (2008) Remote navigation systems in electrophysiology. Europace 10:iii57–iii61